Antibacterial and Alkali-responsive Cationic Waterborne Polyurethane Based on Modification of Aloe Emodin

XIONG Xiaoyan[1,2], LI Xiaobin[1,2], ZHU Zifan[1,2], ZHANG Ending[1,2],
SHI Jun[1,2,4]✉ and LU Mangeng[1,2,3,5]

Cationic water-based polyurethane(CWPU) was synthesized to explore aloe-emodin modifies to obtain CWPU materials with better comprehensive performance. It provides a simple way to synthesize antibacterial waterborne polyurethane, which is to introduce the end-blocking group of herbal extracts into the structure. It contains synergistic antibacterial effect of herbal antibacterial and quaternary ammonium ion on *Escherichia coli*. It makes the material resist the erosion of bacterial, and increase the service life of materials. When the pH value of the environment changes, the UV absorbance of the aloe-emodin modified cationic water-based polyurethane(AE-CWPU) also changes. Therefore, within a certain detection range, AE-CWPU has great applications in the field of smart response materials. The modified thermodynamic properties have been improved, and the mechanical properties basically maintained the maximum stress, and the elongation at break was reduced.

Keywords Waterborne polyurethane; Aloe emodin; Quaternary ammonium salt; Antibacterial; pH response

1 Introduction

As COVID-19 spreads globally, people pay more attention to the impact of microorganisms on human life whether viral or bacterial[1]. Materials with antibacterial properties achieve sterilization or antibacterial properties by contacting sterilization[2] or inhibiting the reproduction of microorganisms on the surface[3]. Polymer materials with antibacterial properties are not only conducive to human daily needs, but also form a delicate balance with microorganisms[4]. It is also beneficial to prolong the service life of the material itself and conducive to long-term protection as a coating[5]. Compared with the usual need to spray antiseptics or sterilizers, modifying the material itself with antibacterial properties can achieve a "once and for all" effect. Antibacterial

✉ SHI Jun
junshi@gic.ac.cn
1. Guangzhou Institute of Chemistry, Chinese Academy of Sciences, Guangzhou 510650, P. R. China;
2. University of Chinese Academy of Sciences, Beijing 100049, P. R. China;
3. Guangdong Provincial Key Laboratory of Organic Polymer Materials for Electronics, Guangzhou 510650, P. R. China;
4. New Materials Research Institute of CASCHEM(Chongqing) Co., Ltd., Chongqing 400714, P. R. China;
5. CASH GCC Shaoguan Research Institute of Advanced Materials, Shaoguan 512440, P. R. China

is a key material property. Some of the current antibacterial studies are modified by silver elements, such as carbon fiber composite silver[6], silver chelate[7], silver nanoparticles[8] or nanowires, silver mosaic two-dimensional materials[9]. It has the characteristics of high price and insufficient degradation[10]. Another is modified by silicon elements[11], which is characterized by a cheap price and easy cracking, and sometime rough surface is conducive to the adhesion of bacteria[12]. Others are modified by titanium-based metals with high cost and poor compatibility[13].

The matrix waterborne polyurethane is a novel type of environmentally friendly polymer material. Water-based polyurethane is non-combustible, low toxicity, non-pollution, and highly workable. It also has flexibility and resistance to solvent-induced swelling, solubility, cracking or warping. Cationic waterborne polyurethane is a kind of waterborne polyurethane, which has cationic groups on its skeleton with some unique properties. The main chain of cationic waterborne polyurethane has tertiary amine groups or sulfonium groups and other hydrophilic groups[14]. It is used in glass, leather[15], and coatings[16]. According to the mechanism of cationic immobilization of cell membrane, it has its own antibacterial effect. In addition, the structure of cationic waterborne polyurethane has a positive charge[17], which is equal to the dust in the air. Due to the principle of magnetic homogeneous repulsion, it has anti-dust effect. Aloe-emodin is a natural herbal extract that causes little harm to the environment when it degrades[18].

With the development of science and technology, environmental stimulus response materials are increasingly in demand in the fields of smart materials, coatings, sensing, catalysis, nanotechnology and biomedicine[19−24]. The anthraquinone structure of aloe-emodin(AE) undergoes reciprocal isomerization upon pH change. When the environment is acidic, AE exhibits an anthraquinone structure with visually red. Under alkaline conditions, AE exhibits an anthracene structure with a macroscopic yellow and orange color. Within a certain detection range, aloe-emodin cation water-based polyurethane(AE-CWPU) has potential applications for promotion in the field of smart responsive materials. AE with a wide range of antibacterial

effects is 1,8-dihydroxy-3-hydroxymethylanthraquinone, coplanar with three rings. It is easy to enter bacteria and make their metabolism slow, and the hydroxyl group on the anthraquinone structure can make bacteria apoptosis[25−30].

Based on CWPU, the antibacterial effect of its quaternary ammonium salt, combined with the antibacterial properties of AE, is used to achieve synergistic antibacterial effect. The addition of AE to CWPU improved the thermodynamic properties and maintained the pH response properties[31]. Since AE itself is poorly water-soluble and hardly soluble in water, if it is simply mixed physically, phase separation may occur, and a stable structure may not be formed. In this study, CWPU is modified by the molecular structure design, and it is expected to prepare a stable CWPU emulsion[32].

2 Experimental

2.1 Materials

Polyethylene glycol-600, hexamethylene diisocyanate(HDI, 99.0%) and isophorone diisocyanate(IPDI, 99%) were purchased from Shanghai Macklin Biochemical Technology Co., Ltd.(Shanghai, China). Toluene diisocyanate(TDI) of industrial grade, acetone of analytical purity and anhydrous ethanol were from Guangzhou Chemical Reagent Factory (Guangzhou, China). Dibutyltin dilaurate solution(95%) and N-methyldiethanolamine(MDEA, 99%) were purchased from Shanghai Aladdin Biochemical Technology Co., Ltd.(Shanghai, China). 1.8-Dihydroxy-3-hydroxymethyl anthraquinone(AE, 95%) was purchased from Shaanxi Haochen Biotechnology Co., Ltd.(Xi'an, China). Glacial acetic acid of analytical purity was purchased from Jiangsu Qiangsheng Functional Chemical Co., Ltd.(Changshu, China). Deionized water of analytical pure was purchased from Guangzhou Ruijian Instrument Co., Ltd.(Guangzhou, China).

2.2 Synthesis of AE-CWPU, AE&CWPU and CWPU

AE-CWPU was synthesized according to a stepwise reaction method[33]. To a 500 mL four-neck flask containing acetone (20.00 g), polyethylene glycol-600(20.00 g) and toluene diisocyanate(8.75 g) were added. The stirring speed was then set to 200 r/min, the reaction temperature was increased to 75 °C, and upon adding two and three drops of dibutyltin dilaurate to the solution, it was observed that the temperature of the thermometer inserted in the flask reached >60 °C. Subsequently, the solution was heated for 1 h, after which MDEA(0.70 g) and acetone(10.00 g) were added, and heating of the reaction mixture was continued for 1.5 h. AE(0.2147 g,

solid content of 0.38%) was dissolved in acetone(20.00 g) and heated for 2 h. After this time, the reaction mixture was quickly cooled to a temperature not exceeding 35 °C and glacial acetic acid(0.3523 g) was added before stirring was continued for 0.5 h. After this time, the speed was increased to 1600 r/min and deionized water(70.20 g, 30% solids) was added to the solution for emulsification and stirring was continued at high speed for 0.5 h. Finally, after 24 h, the acetone was removed *via* reduced pressure distillation at less than 40 °C. Then, a film mold was placed on an electronic scale, to which the the emulsion sample was placed, the mass of the sample(error±0.02 g) was recorded, and then it was stored in a ventilated and dust-free place. After drying at room temperature for 24 h, the AE-CWPU films were collected and packed into airtight polythene bags.

As shown in Fig.1, a stepwise method was used in this experiment. The first step involved the reaction of diisocyanate with PEG-600 to form a prepolymer. In the second step, the —OH group of MDEA reacted with the —NCO group of the above prepolymer to further increase its molecular weight. After CWPU with a larger molecular weight was formed, the hydroxymethyl group of AE reacted with—NCO at both ends of the polymer chain. Finally, after the acidification with hydrochloric acid and the emulsification with deionized water, a stable oil-in-water structure was formed.

Synthesis of CWPU: CWPU was used as a control, prepared *via* the stepwise reaction method. The same steps were followed as for AE-CWPU, without the addition of AE, keeping the reaction time, temperature, type of solvent, catalyst, and other constant factors the same.
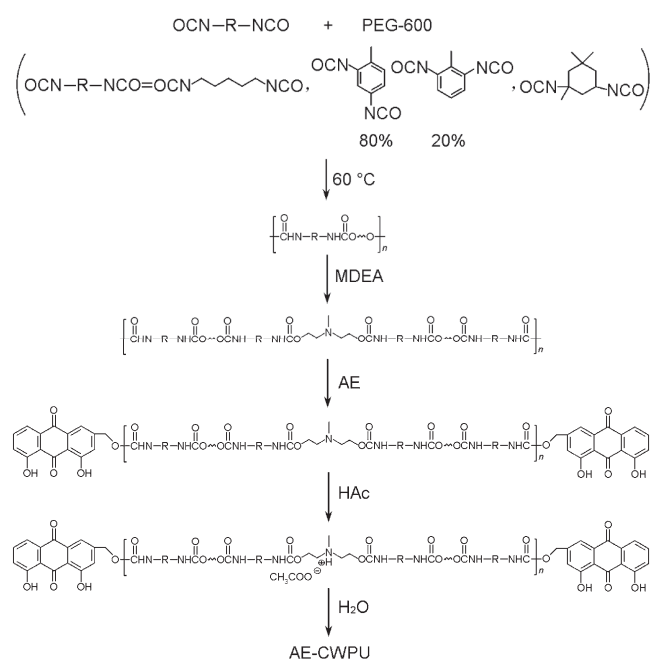

Fig.1 Synthetic route of AE-CWPU

Synthesis of AE&CWPU: first, after collecting the CWPU emulsions, their solid content was recorded, in addition to the mass of AE. Second, AE was added to CWPU and dispersed by magnetic stirring at 200 r/min for 1 h. Third, the solution was ultrasonicated for 1 h, before being dropped into the mold and allowed to dry naturally for 24 h. Finally, sample films were collected in a sealed bag.

2.3 Antibacterial Testing

In terms of bacterial strains, the total number of bacterial colonies was determined according to the People's Republic of China Light Industry Standard QB/T4341-2012 and the People's Republic of China National Standard GB/T4789.2-2003. Second-generation *Escherichia coli*(ATCC25922) strains were purchased from Beijing Biological Collection(Beijing, China). The bacteria used in this experiment passed gram staining, colony characteristic mannitol fermentation, Baird-Parker agar colony characteristic, plasma coagulase, glucose, mannitol, catalase, α-hemolysin, thermostable nucleic acid test enzyme, novobiocin, pyrrolidone-β-naphthylamide, Voges-Proskauer, ornithine decarboxylase, protein A, and 16s rDNA sequencing testing. AE-CWPU, AE&CWPU, and CWPU were sprayed on a 75% solution of ethanol prior to the tests, washed with sterile water for 1 min, and allowed to dry naturally. The petri dishes and other utensils used in the experiments were sterilized *via* a high-temperature damp-heat method for at least 20 min[34,35].

For antibacterial "pancake" testing, the pre-treatment of three sets of samples not only were named as AE-CWPU, AE&CWPU, CWPU, but also prepared three pieces made into a 30 mm × 30 mm square. Prior to the antibacterial experiments, samples were surface sterilized using 70% ethanol for 1 min followed by rinsing with deionized water. The samples were then placed in a constant temperature and humidity apparatus, with the temperature adjusted to 37 °C and the humidity to 20%. Preparation of nutrient agar medium: sodium chloride (5.0 g), soy peptone(10.0 g), and beef extract(5.0 g) were dissolved in distilled water(1000 mL), and the pH was adjusted to 7.0—7.2 using a 0.1 mol/L solution of sodium hydroxide. After completing these steps, the agar(15.0 g) was divided into various petri dishes, which were sterilized in a pressure steam sterilizer at 120 °C for 20 min. After this time, the agar nutrient medium samples were removed from the sterilizer and allowed to cool for 2 h. A sterile cotton swab was then dipped in a second-generation *Escherichia coli*(ATCC25922) strain with a concentration of 5×10⁷ CFU/mL and used to draw a "pancake" picture on the prepared round agar medium, where 5—7 parallel horizontal lines and 5—7 parallel vertical lines were drawn to make the sample appear as uniform and coordinated as possible, to eliminate the squeezing effects of gravity on the

membrane that would be exerted on the bacterial solution. Afterward, the sample to be tested was placed in the center of the "pancake" picture, and the samples were then put in a constant temperature and humidity apparatus with the temperature set to 37.0 °C and the humidity to 90.0%. Photographs were taken at 0, 16, 24, and 32 h respectively, as well as the antibacterial material being removed and photgraphed after 24 h. By monitoring the *Escherichia coli*(ATCC25922) strain on the antibacterial material over time, its antibacterial performance was determined. The antibacterial "pancake" test plays a qualitative role, as well as a pre-experimental role, in the subsequent determination of the antibacterial rate of the antibacterial material.

Antibacterial rate: uniformly contact between the sample and the bacteria was achieved *via* a patching film method by quantitatively inoculating the bacteria on the antibacterial and blank control materials. After around 24 h of incubation, the number of surviving bacteria in the sample was detected and the antibacterial rate of the sample was calculated. An eluent of physiological saline(0.80%) was added to a 0.10% volume fraction of poly-oxyethylene sorbitan monooleate(Tween-80) surfactant, the pH was adjusted to 7.0—7.2, and the mixture was then sterilized in a high-temperature autoclave at 120 °C for 20 min. Preparation of the bacterial suspension: viable bacteria were calculated according to GB/T4789.2, and an inoculation loop was used to take 1 loop of fresh bacteria from the second-generation culture. In this saline culture solution, a solution of the bacteria was sequentially diluted ten-fold to a concentraion of 5.0×10⁵ CFU/mL. Next, antibacterial testing was conducted. Firstly, similar to the above samples, antibacterial test samples were tested and the blank sample was soaked in a 75% solution of ethanol solution for 1 min, rinsed with sterile water, dried naturally, and placed in a sterilized petri dish. Afterwards, a suspension of the bacteria (0.2 mL) was dropped onto the antibacterial and the blank samples, with three parallel tests conducted for each group of samples. Following this, the sterile samples were picked up with sterilized tweezers and placed on the antibacterial material and the blank material, so that the bacterial suspension could make even contact with the antibacterial and the blank samples. Preceding this, the petri dishes were covered and incubated for (24±1) h at (37±1) °C at a humidity of >90%. Finally, the samples were removed from the incubator and added to the eluate(20 mL), before repeated washing of the tested antibacterial and blank samples and the film, and the above eluate was inoculated in nutrient agar medium with a 10-fold gradient. After 24—48 h of incubation at (37±1) °C, the number of live bacteria in the eluate after being exposed to the antibacterial materials was determined according to the method specified in GB/T4789.2, and the survival rate of bacteria in the liquid was compared *via* the elution of the blank

and antibacterial samples. The data are valid if they meet the following requirements. Firstly, the viable bacteria values of the three parallel samples in the same group must have a (highest log value-lowest log value)/average log value of ≤0.20. Secondly, the recycled number of recovered viable bacteria blank samples must be ≥$1.0×10^4$ CFU/piece. If these requirements are met, the antibacterial rate can be calculated according to Equation (1):

$$R(\%)=[(B−A)/B]×100\% \tag{1}$$

where R is the antibacterial rate; B is the average number of bacteria recovered in blank sample(CFU/piece); and A is the average number of bacteria recovered in the antibacterial test sample(CFU/piece).

Antibacterial fatigue: fatigue is generally a mechanical property, referring to how long a maximum stress can be applied without damaging the material, with examples including engineering mechanics fatigue, mechanical fatigue limit, tensile fatigue, and compression fatigue. Herein, the concept of antibacterial fatigue is porposed, which means that the same antibacterial material is subjected to multiple antibacterial uses, where the antibacterial performance maintained can be defined as 100%—0%, of which 100% indicates non-antibacterial fatigue and 0% refers to extreme antibacterial fatigue. Three sets of antibacterial fatigue experiments were set up to test the antibacterial rate of the three samples for their first use, then the three samples were recovered and the second antibacterial experiment was performed, whereafter their antibacterial rate was recorded. The three samples were then again recovered, and a third antibacterial experiment was performed on them, with their antibacterial rates again recorded. The antibacterial rates of the recovered samples were then compared with the antibacterial rates of the first antibacterial experiment to calculate the antibacterial fatigue. Equation (2) was used to calculate the antibacterial fatigue as follows:

$$\text{Antibacterial fatigue}(\%) = \frac{\text{Recycling antibacterial rate}}{\text{First antibacterial rate}}×100\% \tag{2}$$

2.4 Characterization

After two months of storage, no solid deposition was observed in AE-CWPU, while AE&CWPU showed obvious solid deposition after two months of storage. Two samples(8.0 g) were selected for this study, which were photographed and recorded before centrifugation. A centrifuge(desktop high speed TG16-WS centrifuge, Hunan Xiangli Scientific Instrument Co., Ltd., Changsha, China) was preheated for 10 min prior to the centrifugation of the samples, with the total mass of the samples plus the sealing film, tubes, and lids not exceeding ± 0.01 g. The samples were placed symmetrically in the centrifuge and centrfuged at 9000 r/min for 0.5 h.

Fourier-transform infrared(FTIR, TENSOR27 infrared spectrometer, Bruker, Germany) spectroscopy was used to investigate the AE-CWPU, AE&CWPU, and CWPU polymer sample films based on their different monomers, *i.e.*, toluene diisocyanate, isophorone diisocyanate, and methyl diisocyanate. The samples were scanned over a wavelength range of 4000—400 cm^{-1}, at a resolution of 4 cm^{-1}, with the number of scans set to 16. The content of AE may also overlap with the burr peak. FTIR spectroscopy was mainly used to observe whether AE has an effect on the formation of base groups and if it destroys the basic structure of CWPU.

Scanning electron microscopy(SEM, Zeiss Sigma 300) was conducted on 48 h freeze-dried samples that were sprayed with platinum using a platinum target prior to the measurements and scanned with a Schottky field emission electron gun. The microscope was equipped with an energy-dispersive spectroscope(EDS, Smartedx), which was used to conduct EDS mapping of AE-CWPU at 2000× magnification to analyze the types and contents of the elements in the samples to a depth of around 1 μm.

Nuclear magnetic resonance spectroscopy measurements were conducted on a Bruker 400M spectrometer using deuterated dimethyl sulfoxide as the solvent.

Thermogravimetric analysis(TGA, Netzsch TG 209F1, Germany) was conducted at a heating rate of 10 °C/min from 30 °C to 700 °C under a nitrogen atmosphere.

Tensile measurements(Guangdong Yuelian Instrument Co., Ltd., Dongguan, China) were conducted on films with dimensions of 30 mm×10 mm×1 mm at a machine clamp distance of 10 mm, with the program set to stretch the samples at 20 mm/min.

pH response measurements were conducted as follows. First, pharmaceutical-grade sodium hydroxide and 1 mol/L hydrochloric acid were used to prepare pH 1 to 14 standard solutions. The pH values of the solutions were then tested using pH test paper and colorimetric card placed on a white background. Under natural light, each pH standard solution was tested using the pH test paper and colorimetric card. If the difference in color was large, the solutions were repreparad. Special attention was paid to ensure even ten-fold dilution of the solutions. The surface of AE-CWPU with the toluene diisocyanate monomer(mass fraction of AE of 0.38%) was first sprayed with medical alcohol and deionized water and allowed to dry in air. Sodium hydroxide solutions(pH 7—14) were then dropped onto the sample, and a photograph was taken after 30 s. Cotton was then used to absorb the excess of the standard solutions and then another photograph was taken after 30 s. Hydrochloric acid solution(pH=1) was then dropped on each sample to achieve neutralization, with another photograph taken after 30 s.

3 Results and Discussion

3.1 Preparation and Characterization of AE-CWPU, AE&CWPU and CWPU

After centrifugation, it is found that AE-CWPU had no phase separation, while AE&CWPU showed very obvious phase separation as shown in Fig.2(A). Compared with the common "one pot end" synthesis method, this experiment achieves the control of the molecular structure through a step-by-step reaction. This research designs the molecular structure level modification CWPU route. Firstly, to form a prepolymer with a shorter molecular chain, the initial reaction was proceeded by adding diisocyanate and diol. After a period of time, MDEA is used to carry out a chain extension to double its molecular weight and cationic hydrophilic groups are introduced into the polymer chain. Along the middle to late stages of this growth trend, AE made mono terminated or dual terminated forms. The vast majority of those involved in the reaction were the more active hydroxymethyl groups on AE. The highlights of designs are as follows: firstly, the "step-by-step synthesis" has a smaller δ value for the Gaussian distribution of the chain length of the polymer chain than the "one-pot" synthesis method, and the molecular weight is more concentrated. Secondly, most of the hydroxyl groups involved in the reaction of AE are highly active hydroxymethyl groups. The anthracenol group, which has an antibacterial effect in AE, is not destroyed.

There were quite a few solids in the lower layer, and the upper emulsion became more transparent after centrifugation. According to the research[36], the correlation formula[Eq.(3)] between the water solubility of AE and the temperature can be used as a reference.

$$\ln x = 213.08 - 15178.134/T - 30.914\ln T \tag{3}$$

The calculated water-solubility of AE at 25 °C is 8.59×10^{-7}, which is poor in water solubility. Since CWPU has formed a stable oil-in-water structure, AE does not disperse well in CWPU when it is physically blended with CWPU.

AE-CWPU is successfully modified at the molecular structure level of the polymer chains. Deionized water emulsifies it to form a stable oil-in-water structure, and AE-CWPU has a uniform particle size distribution with no phase separation. However, the stratification of AE&CWPU indicates that the water dispersibility of AE is very poor. AE is too hydrophobic to physically blend to form the stable structure of oil-in-water and there appears phenomenon of phase separation.

In addition to the macrostructure, it is also necessary to examine its stability from the microstructure. As shown in Fig.2(B), the highest peak appeared at the beginning of δ 3.5, and each sample almost overlapped, indicating that the urethane bond is successfully synthesized with high intensity. Furthermore, AE-CWPU has two peaks in δ 1.2—1.4, indicating that the carbon atom bonded to polyurethane has a hydrogen atom coupled to its adjacent carbon, resulting in a relatively small chemical shift and a stable component.
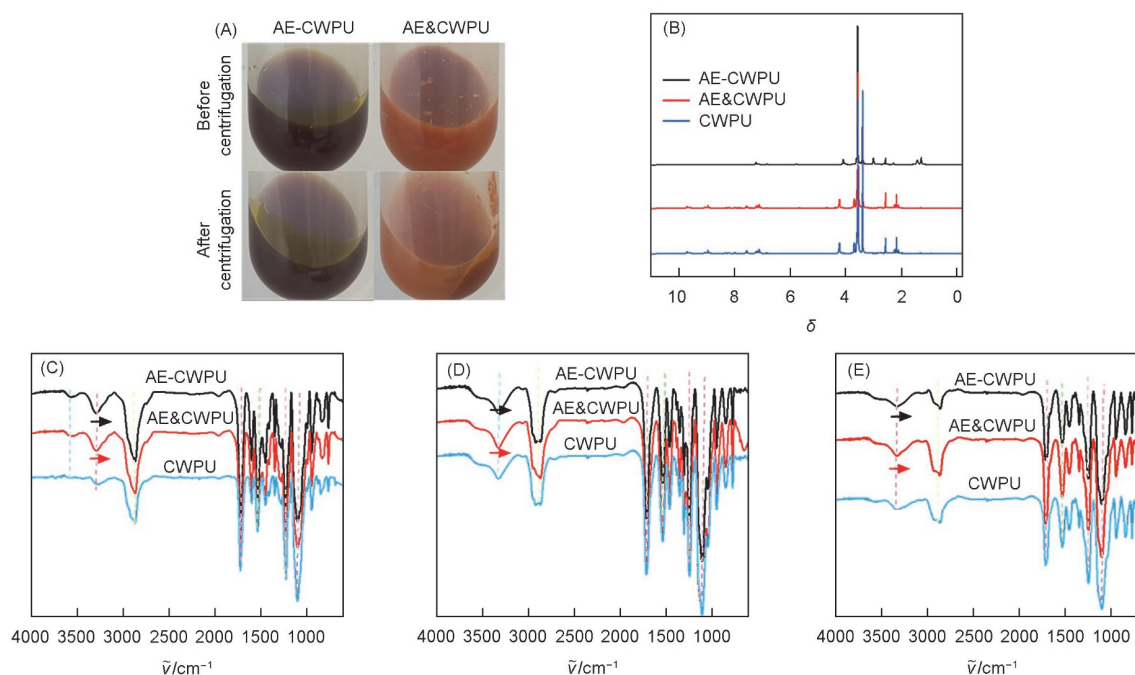

Fig.2 AE-CWPU and AE&CWPU emulsion before and after centrifugation(A), ¹H NMR spectra of AE-CWPU, AE&CWPU, CWPU(B), FTIR spectra by AE-CWPU, AE&CWPU, and CWPU with monomers of TDI(C), IPDI(D) and HDI(E)

The FTIR results in Fig.2(C)—(E) show that the strength of the OH stretching vibration peak near 3300 cm^{-1} has not changed. With the addition of AE, the OH stretching vibration peak is slightly red shift, indicating that it has intermolecular hydrogen bonds. C—H stretching peak is near 2800 cm^{-1}, and the intensity of the stretching vibration peak has not changed. For the carbonyl stretching peak of the urethane bond near 1700 cm^{-1}, there is no red shift or blue shift due to the addition of AE. The strength of the N—H in-plane bending vibration nearby at 1550 cm^{-1} was not changed due to the modification of AE and physical blending. The peak of C—O stretching vibration is near 1250 cm^{-1}, and the strength has hardly changed. And for the C—O—C stretching, the vibration peak is near 1250 cm^{-1}, and three types of three groups of samples do not change much. C—C stretching vibration peak is at about 1140 cm^{-1}. In summary, it can be considered that the introduction of AE did not destroy the basic structure of cationic waterborne polyurethane, and produced a minor amount of intermolecular hydrogen bonds, resulting in a more stable structure. In the latter procedure, thermodynamic properties were further used to determine if a small amount of hydrogen bonds formed.

The formation of substances can be determined by the characteristic functional groups. On this basis, the SEM-EDS can be used to determine whether the element distribution is uniform.

It can be seen from Tables 1 and 2 that the quantification of the surface element distribution of AE-CWPU and AE&CWPU is not completely consistent. According to formula (4),

$$\text{Mass fraction of oxygen element(\%)=} \frac{\text{Mass of oxygen element}}{\text{Total mass of all elements}} \times 100\% \quad (4)$$

the mass fraction of oxygen in aloe-emodin is 29.6%, the mass fraction of oxygen in MDEA is 26.89%, and the mass fraction of the repeated unit $\left[\begin{smallmatrix} O \\ \parallel \\ CHN-R-NHCO\sim O \end{smallmatrix} \right]_n$ is 0.744%.

According to the calculations, among all the polymer disassembly structures, the mass fraction of oxygen element in AE is the largest. Therefore, the mass fraction of oxygen in Table 2 is larger than that in Table 1. That is to say, the amount of AE in Table 2 is higher than that in Table 1. It is verified the conjecture that AE was floated on the AE&CWPU surface in the form of agglomeration when it is naturally air-dried. Therefore, the distribution density of AE on the surface is relatively high. AE&CWPU surface has a higher AE concentration, so it is speculated that its antibacterial effect will be slightly higher.

Table 1 SEM-EDS diagram of AE-CWPU*

Element	Mass fraction(%)	Atomic fraction(%)	Error(%)	Net integer factor	K-layer electron ratio	Z	A	F
C	45.61	52.08	4.09	1065.15	0.3913	1.0306	0.8326	1.000
N	10.58	10.36	9.79	95.09	0.0392	0.9970	0.3719	1.000
O	43.81	37.56	7.42	659.28	0.2205	0.9683	0.5199	1.000

* *Z*: Atomic number correction factor; *A*: absorption correction factor; *F*: fluorescence correction factor.

Table 2 SEM-EDS diagram of AE&CWPU*

Element	Mass fraction(%)	Atomic fraction(%)	Error(%)	Net integer factor	K-layer electron ratio	Z	A	F
C	44.40	50.94	4.18	801.08	0.3790	1.0317	0.8275	1.000
N	9.54	9.39	9.97	67.96	0.0361	0.9980	0.3792	1.000
O	46.06	39.67	7.31	552.80	0.2382	0.9683	0.5335	1.000

* *Z*: Atomic number correction factor; *A*: absorption correction factor; *F*: fluorescence correction factor.

3.2 Morphology

As shown in Fig.3, when magnified 200×, the picture of AE-CWPU has a flat structure, while AE&CWPU has a wavy texture. When magnified at 1000×, the electron micrograph of AE-CWPU is uniform and flat without impurities, while there is a lot of small white dots suspended on the surface of the AE&CWPU sample. When magnified to 5000×, the particle size of the surface of the electron microscope image of AE-CWPU is uniformly distributed, while the electron microscope image of AE&CWPU has many white dots on the surface. According to the diameter of the small white dots, it can be concluded that AE is suspended on the surface of the AE&CWPU sample in the form of agglomeration, and the surface of AE&CWPU also has corresponding dry cracking. When the sample is formed into a film, the surface structure appears uneven and rough.
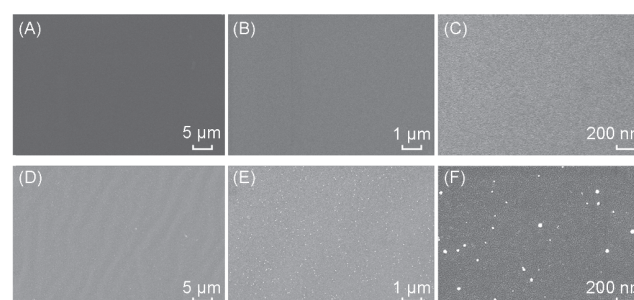

Fig.3 Surface structures of AE-CWPU(A—C) and AE&CWPU (D—F) samples under SEM with different magnifications

The mapping magnification of SEM combined with AE-CWPU is 2000×. It looks almost flawless and the material surface is very uniform and flat. Fig.4(A) is a composite picture of the distribution of carbon, nitrogen and oxygen elements obtained after combined mapping. It can be seen that the pixel points of various colors are relatively evenly distributed. There is a dot in the middle, and the number of three elements is relatively small. Surface depressions due to very small air bubbles or nanoscale dust are difficult to avoid during film formation. Fig.4(B) is a image of the carbon element in the composite element diagram. It can be seen that the distribution of carbon elements on the surface of the material is relatively uniform, and the content is relatively large. Fig.4(C) is a image of the nitrogen element in the composite element diagram. It can be seen from the figure that the distribution of nitrogen on the surface of the material is a relatively dispersed and uniform with a relatively low content. Fig.4(D) is the oxygen element in the composite element mapping. The distribution of oxygen element on the surface of the material is relatively uniform and dense with relatively large content. Therefore, the element distribution of AE-CWPU membranes is uniform.
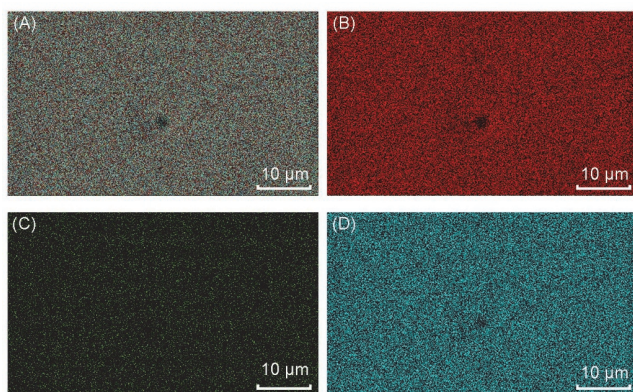

Fig.4 SEM image combined with mapping of AE-CWPU
(A) Composite picture; (B) C; (C) N; (D) O.

3.3 Thermodynamic Stability and Stretch Resistance

As shown in Fig.5(A), on one hand, when the thermal mass loss is 5%, the temperatures of CWPU, AE&CWPU and AE-CWPU are 119.47, 127.42, and 270.16 °C, respectively. On the other hand, when the thermal mass loss is 10%, the temperatures of CWPU, AE&CWPU and AE-CWPU are 263.47, 295.42 and 319.66 °C, respectively. It shows that the introduction of AE increased the temperature at 5% and 10% mass loss. The addition of AE can improve its thermodynamic properties, which is consistent with the results of the previous FTIR inference. It creates intermolecular hydrogen bonds and increases the thermodynamic stability of the material. When
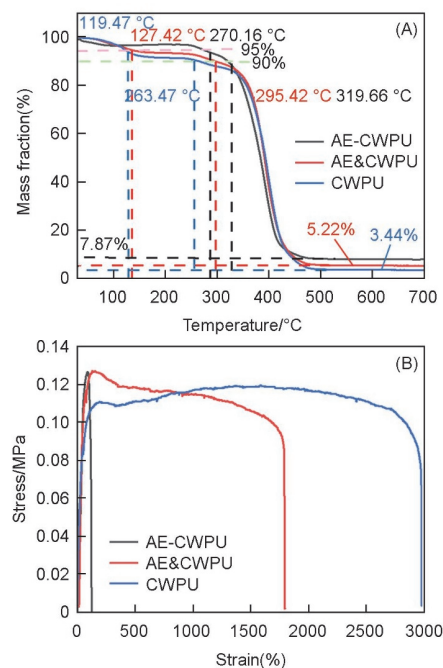

Fig.5 5% and 10% thermogravimetry curves of AE-CWPU, AE&CWPU and CWPU(A) and stress-elongation curves of AE-CWPU, AE&CWPU and CWPU(B)

the temperature is 700 °C, the residual carbon rates of CWPU, AE&CWPU and AE-CWPU are 3.44%, 5.22% and 7.87%, respectively. This indicates that AE-CWPU is resistant above 700 °C and has a higher carbon residual rate.

As shown in Fig.5(B), the maximum stress value of CWPU is 0.115 MPa, and the elongation at break is about 3000%. However, the maximum stress value of AE&CWPU is 0.128 MPa, and the elongation at break is about 1600%. And the maximum stress value of AE-CWPU is 0.128 MPa, and the elongation at break is about 180%. It can be indirectly explained that mechanical properties of AE modified CWPU are reduced. Compared with CWPU, AE&CWPU reduces the elongation at break, and AE-CWPU reduces greatly the elongation at break, but the maximum stress value of AE-CWPU is increased. From the manufacturing process, the introduction of AE in CWPU reduces the molecular weight of the entire material, so the tensile performance of the material is not good.

3.4 Antibacterial

As shown in Fig.6, the bacterial was inoculated and grew normally until 16 h. The number of bacteria was kept at a steady state and was used as a blank control for the next three groups. In the CWPU group, the bacteria grew normally for 16 h. In the area covered by the CWPU film, the growth of the bacterial colonies was slowed down or even inhibited, as seen
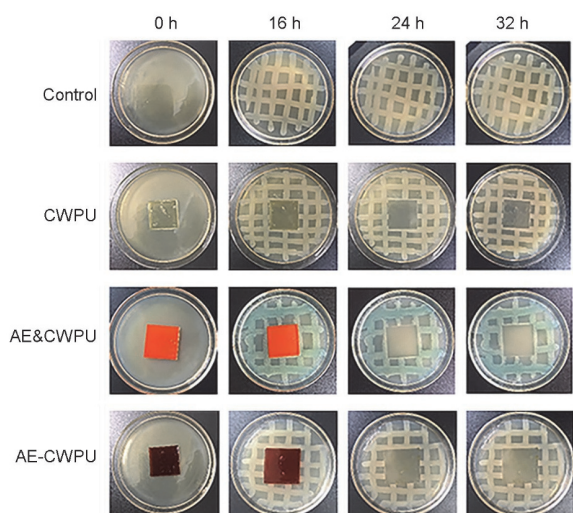
Fig.6 CWPU, AE&CWPU, and AE-CWPU covered with the "pancake" picture of *Escherichia coli*

by the transparent CWPU. Then, the CWPU was removed after 24 h. Due to the viscosity of the membrane, a small part of the bacterial colonies were taken away, and a part of the bacterial colonies remained. After another 8 h of cultivation, it was found that the bacterial colony continued to multiply, indicating that CWPU has limited antibacterial effect. The bacterial in the AE&CWPU group grew normally for 16 h. In the area covered by AE&CWPU film, its antibacterial properties could not be observed, so the film was to be removed after 24 h. Petri dishes were incubated for 8 h and found to be almost no bacterial flora, indicating that AE&CWPU has a strong antibacterial effect. The bacterial in the AE-CWPU group grew normally for 16 h. In the area

covered by AE-CWPU film, its antibacterial properties could not be directly observed. When the film was removed for 24 h, almost no bacterial remained. After culturing for another 8 h, only a few small bacterial groups have grown, indicating that AE-CWPU also has a relatively strong antibacterial effect.

According to experimental results, the calculated antibacterial rate can be seen as shown in Fig.7(A). Antibacterial rates of CWPU, AE&CWPU and AE-CWPU are about 46.8%, 54.8% and 55.2%, respectively. It can be seen from the above that the introduction of AE into CWPU can increase its antibacterial rate by about 8%—10%. Therefore, AE can be modified by chemical or physical blending and effectively improve the antibacterial rate of CWPU. The highest antibacterial rates of CWPU, AE&CWPU and AE-CWPU are 47.3%, 57.8% and 55.6%, respectively. The highest antibacterial rate of CWPU with AE is higher than that of CWPU.

It can be seen from Fig.7(B) that the antibacterial rate has a corresponding decrease when the antibacterial materials are recycled. Among them, the antibacterial rates of CWPU and AE-CWPU have a similar decreasing tendency, indicating that it has a tiny value antibacterial fatigue. However, the antibacterial rate of AE&CWPU has a relatively large decline, indicating that it has antibacterial fatigue.

Antibacterial mechanism is shown in Fig.7(C). The quaternary ammonium salt on the cationic waterborne polyurethane backbone has a certain antibacterial effect by electrostatically attracting negative electrons on the surface of the *Escherichia coli* cell membrane. AE is most sensitive to the inhibitory effect of *Staphylococcus*, *Streptococcus*, and *Escherichia coli*. The mechanism of antibacterial is that the tricyclic coplanar cuts into the bacteria to inhibit the electron
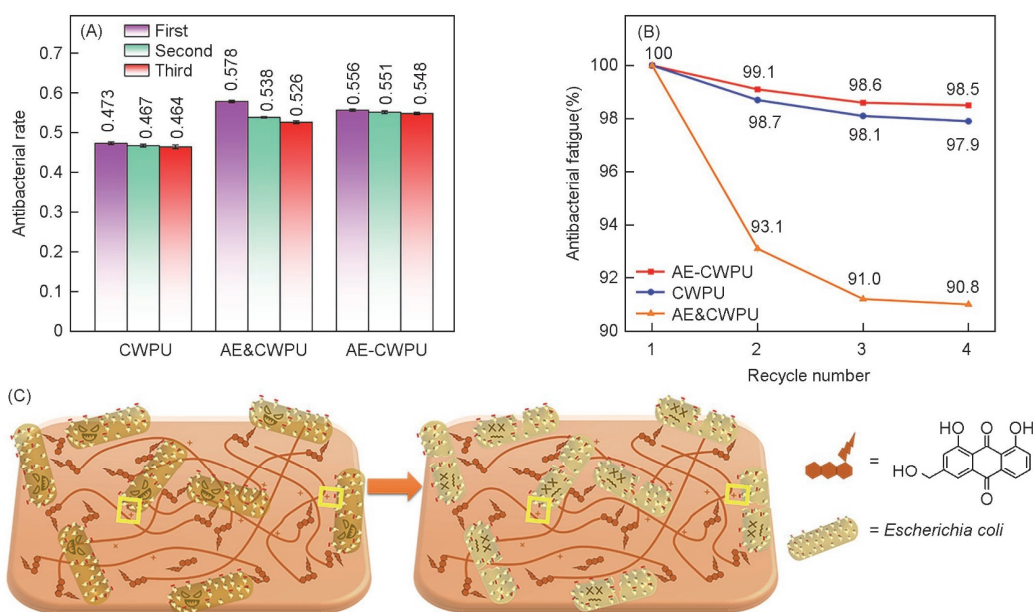

Fig.7 First, second and third time antimicrobial rates(A) and antibacterial fatigue(B) of CWPU, AE&CWPU and AE-CWPU, and synergistic antibacterial mechanism of Aloe rhodopsin and cationic group(C)

transport in the mitochondrial respiratory chain, and strongly inhibits the synthesis of nucleic acid and protein. Synergistic antibacterial effect is that the quaternary ammonium salt group fixes the bacteria on the surface of the antibacterial material, helping AE to enter the bacteria to inhibit the mitochondrial transfer material, and bring out a small part of the bacteria content. It increases the negative electron concentration per unit area of the bacteria membrane. So the electrostatic attraction of cations is enhanced, thereby enhancing the antibacterial effect of the quaternary ammonium salt cationic group.

As shown in Tables 2 and 3, SEM-EDS surface semi-quantitative results are about AE&CWPU samples and their recovered antibacterial tests samples. The percentages of carbon element, nitrogen element and oxygen element are 45.01%, 10.01% and 44.98%, respectively. However, the recovered sample(44.98%) had less oxygen than the original sample(46.06%), indicating that the content of AE on the surface of the recovered sample has become smaller, confirming the antibacterial fatigue conjecture. AE on the surface of AE&CWPU was lost during the recycling process. This distribution density of AE on the membrane surface decreases, resulting in a decrease in antibacterial rate. In addition, AE and CWPU are physically blended, and the combination is not tight enough, so it is easier to reflect antibacterial fatigue.

Analyzing the experimental results, there are two reasons for the fatigue of antibacterial materials. Firstly, the surface of the recycled antibacterial materials inevitably has corresponded losses during the recycling process. The comparison of CWPU also shows that the recycling process inevitably generates antibacterial fatigue. Secondly, the structure of AE-CWPU is more stable to form a chemical bond. Therefore, when recycled and used, AE-CWPU has a slight antibacterial fatigue, similar to CWPU. However, AE with poor water solubility was floated on the surface, resulting in a relatively large distribution density of AE on the surface of AE&CWPU. Because the initial antibacterial rate is relatively large, and when it is recycled, part of AE is washed away by the highly soluble ethanol reagent. The surface structure of AE&CWPU was observed by SEM to verify that the distribution density of local AE on the surface of AE&CWPU was relatively large. Semi-quantitative analysis was performed by SEM combined with mapping to verify the change of the AE distribution density on the surface after recovery.

Table 3 SEM-EDS diagram of recycling AE&CWPU*

Element	Mass fraction(%)	Atomic fraction(%)	Error(%)	Net integer factor	*K*-layer electron ratio	*Z*	*A*	*F*
C	45.01	51.30	4.11	1033.19	0.3882	1.0304	0.8306	1.000
N	10.01	9.87	9.80	82.63	0.0367	0.9971	0.3745	1.000
O	44.98	38.83	7.24	600.47	0.2264	0.9686	0.5231	1.000

* *Z*: Atomic number correction factor; *A*: absorption correction factor; *F*: fluorescence correction factor.

3.5 pH Sensitive Response

As shown in Fig.8(A), the first row is the colors of AE-CWPU in standard solutions with different pH values. The second row is the colors of AE-CWPU dried with cotton after contacting with standard solutions with different pH values. And the third row is the colors of AE-CWPU under neutralization of hydrochloric acid. It is shown that AE-CWPU can change color in response to different pH values in wet or dry environments and can return to its original color by neutralization reaction. As shown in Fig.8(B), AE-CWPU is uniformly contacted with standard solutions with pH values of 4 to 14. Then the values of absorbance corresponding to different wavelengths in the ultraviolet-visible spectrum of AE-CWPU are tested. It is shown that AE-CWPU has different absorbance at different pH values with corresponding regularity in detection range, and has prospect in the field of smart reactive materials.

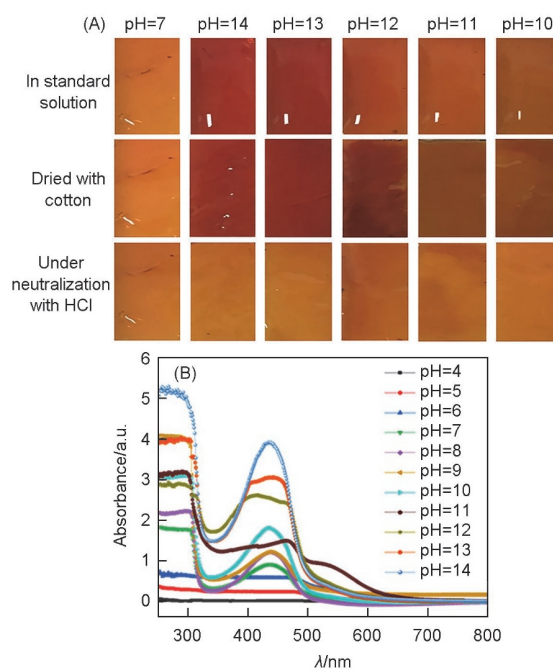AE monomer changes its color by changing the pH value in the environment[37]. As shown in Fig.9, in an alkaline

Fig.8 Colors of AE-CWPU with different pH values(A) and UV absorption spectra of AE-CWPU with different pH values(B)

environment, the anthraquinone structure of AE becomes an anthraphenol structure. The stronger the alkalinity of environment, the more complete the reaction is. The ratio of anthraquinone to anthraquinol structure is influenced by pH value. Therefore, it appears different colors macroscopically. The hydroxymethyl group of AE reacts with the —NCO of CWPU to obtain AE-CWPU, and retains the color changing group of AE.
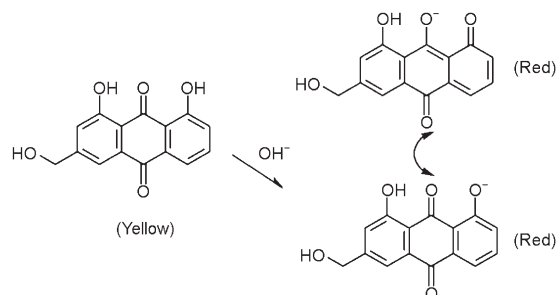

Fig.9 Principle of pH response color about AE

4 Conclusions

In this work, CWPU was obtained by "step by step" method. On the basis of its own antibacterial rate of about 47%, the introduction of a mass fraction of 0.38% AE increased the antibacterial rate by nearly 10% with hardly antibacterial fatigue. In people's stereotypes, most herbal plant extracts lose their activities at high temperatures, thus affecting antibacterial properties. However, this experiment is compared by heating chemical modification and physical blending, and confirmed that CWPU modified by AE maintains antibacterial performance even at a temperature of 60 °C. It is hoped that it can provide a reference for the exploration of adding other herbal extracts to water-based polyurethane. And 0.38% AE modified CWPU can make pH response more obvious when observed by the naked eye. In ultraviolet spectroscopy, AE-CWPU acts as a bridge to convert the pH signal in the environment into a signal of absorbance, so there is a great prospect of application in smart responsive materials. In the FTIR, it was found that the intermolecular hydrogen bonds generated when AE modified CWPU made its molecular structure more stable, but the end capping of AE would reduce the molecular weight and the elongation at break. It is expected that on the basis of maintaining antibacterial performance and pH response performance, its thermodynamic performance can be improved and its practical application field can be expanded.

Conflicts of Interest

The authors declare no conflicts of interest.

References

[1] Jia R. P., Hui Z., *New Journal of Chemistry*, **2020**, *44*, 19759
[2] Yu C. P., Shi C. S., *Biomedical Chromatography*, **2016**, *11*, 3735
[3] Xi J. Q., Wu Q. W., *ASC Biomaterials Science & Engineering*, **2018**, *4*, 4391
[4] Liang H. Y., Lu Q. M., *Chemical Engineering Journal*, **2020**, *421*, 12774
[5] Maurizio V., Federico B., *Material*, **2020**, *13*, 4296
[6] Xing D., Xie Y. X., *Materials & Design*, **2020**, *185*, 108227
[7] Mohammadia A., Doctorsafaeia A. H., *Chemical Engineering Journal*, **2009**, *70*, 363
[8] Cheng L.S., Ren S. B., *Polymer*, **2020**, *12*, 407
[9] Zhu X. Y., Liu P., *Ceramics International*, **2020**, *47*, 173
[10] Madbouly S. A., *Molecules*, **2021**, *26*, 961
[11] Ding X. D., Zhang H., *Materials Today Communications*, **2020**, *23*, 100911
[12] Lu S.Y., Meng G., *Chemical Engineering Journal*, **2021**, *404*, 126526
[13] Wang Y., Li T., *I&EC Researcher*, **2019**, *59*, 458
[14] Liang H. Y., Lu J. Y., *Industrial Crops & Products*, **2018**, *17*, 169
[15] Sukhawipat N., Pasetto P., *Progress in Organic Coatings*, **2020**, *148*, 105854
[16] Huang H. W., Tian Y. Q., *I&EC Researcher*, **2020**, *59*, 15424
[17] Lu Z., Zhang C., *Wuhan University of Technology-Mater*, **2020**, *35*, 832
[18] Li Y., Zhang S. Q., *Applied Polymer*, **2021**, *139*, 51622
[19] Li S. L., Han M., *Journal of the American Chemical Society*, **2019**, *141*, 12663
[20] Ji X. Q., Zhang W., *Progress in Organic Coatings*, **2020**, *145*, 105164
[21] Li J. P., Zhang X. Y., *Polymer Bulletin*, **2015**, *72*, 881
[22] Huang T. W., Lu H. T., *Materials Science & Engineering C*, **2021**, *118*, 111396
[23] Zia J., Mancini G., *Chemical Engineering Journal*, **2021**, *403*, 126373
[24] Wang S. Y., Yang L. P., *Polymer*, **2020**, *12*, 1135
[25] Wu Y. Y., Zhang J. H., *Biochemical and Biophysical Research Communications*, **2017**, *490*, 601
[26] Gao R., Wu X. W., *Onco Targets and Therapy*, **2019**, *12*, 3713
[27] Chen R. E, Wang S. P., *Drug Delivery*, **2014**, *22*, 666
[28] Xiang H., Cao F. J., *Applied Microbiology Biotechnology*, **2017**, *101*, 6671
[29] Shen Y. F., Huang Y., *Reactive and Functional Polymers*, **2020**, *148*, 104486
[30] Feng Z. X., Wang D., *International Society for Biofabrication*, **2020**, *12*, 035015
[31] Meng L. Q., Shi X. Z., *Applied Polymer*, **2020**, *137*, 49314
[32] Duan H. G., Wei Y. H., *Drug Development Research*, **2009**, *70*, 363
[33] Wang Y., Chen R., *I&EC Researcher*, **2019**, *59*, 458
[34] Hosseinabadi Z., Monfared H., *Desalination and Water Treatment*, **2015**, *56*, 2382
[35] Zheng M., Chen J., *Thermodynamics*, **2018**, *127*, 56
[36] Wang C. H., Mu C. D., *Advances in Colloid and Interface Science*, **2020**, *283*, 102235
[37] Gao Y., Zhang X. Y., *Biochemical Pharmacology*, **2021**, *186*, 114476